Equilibrium Point analysis of macro traffic flow model considering the influence of front and rear lights

Ting Zhang[1], *Wenhuan* Ai[1,*], and *Dawei* Liu[2]

[1]College of Computer Science and Engineering, Northwest Normal University, Lanzhou, Gansu, 730070, China
[2]College of Electrical Engineering, Lanzhou Institute of Technology, Lanzhou, Gansu, 730050, China

Abstract. In this paper, the traveling wave solution of the macro continuum model considering the automobile tail lamp effect is obtained by using the phase plane analysis method, the type of equilibrium point of the model is determined, and the stability of the system at the equilibrium point is analyzed. This method can describe and predict the nonlinear traffic phenomena on Expressway from the perspective of system global stability. According to the theory of differential equation, the model is further analyzed to judge the type and stability of equilibrium point. Finally, the simulation diagram is used for numerical simulation. Through numerical verification, it is concluded that the numerical results are consistent with the theoretical analysis.

Keywords: Traveling wave substitution, Stability analysis, Phase plan.

1 Introduction

Since the first [1] car following model was proposed, in order to better describe the movement of cars, various car following models have appeared one after another. For example, Newell [2] developed a car following model with a simple rule. Bando et al. Proposed an optimal speed (OV) model, which can successfully describe some real-time traffic phenomena, such as stop and go, traffic jam, etc. [3]. Later, the OV model was extended, including generalized (GF) model [4] and full velocity difference model (FVD) [5]. FVD model is given as follows:

$$\frac{dv_n(t)}{dt} = a[V(\Delta x_n(t)) - v_n(t)] + \lambda \Delta v_n \tag{1}$$

In recent years, a new point of view on the effect of front and rear lights has emerged to study the impact of front and rear lights on driving behavior [6].

* Corresponding author: wenhuan618@163.com

© The Authors, published by EDP Sciences. This is an open access article distributed under the terms of the Creative Commons Attribution License 4.0 (http://creativecommons.org/licenses/by/4.0/).

The new car following model [7] considering vehicle tail lamp effect established by Zhang et al. Is as follows:

$$\frac{dv_n(t)}{dt} = a[V(\Delta x_n(t)) - v_n(t)] + \lambda \Delta v_n + \theta_n(t)\xi_n(t) \tag{2}$$

The macro traffic model [8] considering the effect of front and rear lights established by Liu et al. Is given as follows:

$$\frac{\partial v}{\partial t} + (v - \lambda\Delta - M\Delta)\frac{\partial v}{\partial x} = a[V_e(\rho) - v] + \frac{1}{2}(\lambda + M)\Delta^2 v_{xx} \tag{3}$$

The model can well reflect the influence of automobile tail lamp on the macro view.

In the second section, the model and its derivation process are discussed. In the third section, the types of equilibrium points of the model are derived, and the stability of the model at different types of equilibrium points is analyzed. In the fourth section, numerical simulation is carried out and the theoretical analysis is verified. The fifth section summarizes the full text.

2 Model and its derivation

Next, we take a new continuum model considering vehicle tail light effect as an example to analyze the branching phenomenon of traffic flow. The model ensures the basic principle of anisotropy of traffic flow and response only to the stimulation of vehicles in front. The model consists of the following two equations, a local vehicle conservation equation,

$$\frac{\partial \rho}{\partial t} + \frac{\partial(\rho v)}{\partial x} = 0 \tag{4}$$

and an equation of motion,

$$\frac{\partial v}{\partial t} + (v - \lambda\Delta - M\Delta)\frac{\partial v}{\partial x} = a[V_e(\rho) - v] + \frac{1}{2}(\lambda + M)\Delta^2 v_{xx} \tag{5}$$

$$\mathrm{M}=\xi_0 \tanh(1-\frac{\Delta}{\mathrm{x}_0}) \tag{6}$$

It is assumed that the model has traveling wave solution $\rho(z)$ and $v(z)$, where $z = x - ct$, traveling wave velocity $c < 0$. sing the above results and bringing them into equations (4) and (5), we can get

$$-c\rho_z + q_z = 0 \tag{7}$$

$$-cv_z + (v - \lambda\Delta - M\Delta)v_z = a[v_e(\rho) - v] + \frac{1}{2}(\lambda + M)\Delta^2 v_{zz} \tag{8}$$

From equation (7):

$$v_z = \frac{c\rho_z}{\rho} - \frac{q\rho_z}{\rho^2} \tag{9}$$

$$v_{zz} = \frac{c\rho}{\rho^2} - \rho_{zz} \tag{10}$$

Then, take (9)-(10) into (8) and rewrite (8), we can get:

$$\rho_{zz} - \frac{2}{(\lambda+M)\Delta^2}\left[\frac{q*}{\rho} - \lambda\Delta - M\Delta\right]\rho_z + \frac{2\rho}{T(\lambda+M)\Delta^2 q*}[q* + c\rho - \rho v_e(\rho)] = 0 \tag{11}$$

Simplify the second order ordinary differential equation about$\rho(z)$:

$$\rho_{zz} - G(\rho, q*)\rho_z - F(\rho, c, q*) = 0 \tag{12}$$

Among them:

$$G(\rho, q*) = \frac{2}{(\lambda+M)\Delta^2}\left[\frac{q*}{\rho} - \lambda\Delta - M\Delta\right] \tag{13}$$

$$F(\rho, c, q*) = -\frac{2\rho}{T(\lambda+M)\Delta^2 q*}[q* + c\rho - \rho v_e(\rho)] \tag{14}$$

Let $\frac{d\rho}{dz} = y$, equation (12) can be transformed into a system of first-order ordinary differential equations:

$$\begin{cases} \frac{d\rho}{dz} = y \\ \frac{dy}{dz} = G(\rho, q*)y + F(\rho, c, q*) \end{cases} \tag{15}$$

3 The balance point type and stability of the mode

The linear representation of the system can be obtained by Taylor expansion of equation (15):

$$\begin{cases} \rho' = y \\ y' = G(\rho_i, q*)y + F'(\rho_i, c, q*)(\rho - \rho_i) \end{cases} \tag{16}$$

Therefore, the Jacobian matrix of the system at the equilibrium point can be obtained as:

$$L = \begin{bmatrix} 0 & 1 \\ F_i' & G_i \end{bmatrix} \tag{17}$$

The corresponding characteristic equation is:

$$\lambda^2 - \mathrm{G_i}\lambda - \mathrm{F_i'} = 0 \tag{18}$$

Where $G_i = G(\rho_i, q*)$ and $F_i' = F'(\rho_i, c, q*)$. From (17) and (18) forms, we can get:

$$F_i' = -\frac{2\rho_i}{T(\lambda+M)\Delta^2 q*}[c - \rho_i V_e'(\rho_i) - V_e(\rho_i)] \tag{19}$$

$$G_i = \frac{2}{(\lambda+M)\Delta^2}\left[\frac{q*}{\rho_i} - \lambda\Delta - M\Delta\right] \tag{20}$$

Since at the equilibrium point $(\rho_i, 0)$,then $q_* + c\rho_i - \rho_i V_e(\rho_i) = 0$,then F_i' can be written as:

$$F_i' = \frac{2\left(q*+\rho_i^2 V_e'(\rho_i)\right)}{T(\lambda+M)\Delta^2 q*} \tag{21}$$

From the Hartman-Gorban linearization theorem, we know that the nonlinear system (15) and the linear system (16) have the same equilibrium point. Select the balance velocity function proposed in:

$$V_e(\rho) = V_f\left\{\left[1 + exp\left(\frac{\frac{\rho}{\rho_m} - 0.25}{0.06}\right)\right]^{-1} - 3.72 \times 10^{-6}\right\} \tag{22}$$

Here, V_f represents the free flow velocity, and ρ_m Represents the maximum density.
The values of the parameters in the model in this chapter are as follows:

$V_f = 30m/s$, $\rho_m = 0.2veh/m$, $a = 0.2$, $\Delta x = 100m$, $x_0 = 100$, $\lambda = 0.6$. From the above discussion and (15)-(16), the type and stability of the equilibrium point can be judged, as shown in Table 1, where the equilibrium point is represented by $\rho_i (i = 1,2,3)$.

Table 1. The equilibrium point.

	ρ_1	ρ_2	ρ_3
	0.0065	0.0938	0.1447
$(c,q) = (-1.371, 0.2)$	$F_i' > 0$, saddle point, unstable for $z \to \pm\infty$.	$\Delta_i < 0, G_i < 0$, spiral point, stable for $z \to +\infty$; unstable for $z \to -\infty$.	$F_i' > 0$, saddle point, unstable for $z \to \pm\infty$.
	0.0223	0.0594	
$(c,q) = (-1.38, 0.64)$	$F_i' > 0$, saddle point, unstable for $z \to \pm\infty$.	$\Delta_i < 0, G_i < 0$, spiral point, stable for $z \to +\infty$; unstable for $z \to -\infty$.	

4 Numerical simulation

The two sets of parameters in Table 1 are selected to simulate the stability of the nonlinear system (15) at the equilibrium point. The phase plan near the balance point is shown in Figure 1 and Figure 2. The equilibrium point is $(\rho_i, 0)$, and $i = 1,2,3$, $\rho_1 < \rho_2 < \rho_3$. It can be seen from the figure that the balance point type of the system and the stability changes near the balance point are consistent with the theoretical analysis results in Table 1.

Figure 1 corresponds to the first situation in Table 1. It can be seen from Table 1 that when $z \to \pm\infty$, the system is unstable at the equilibrium point $(\rho_1, 0)$ and $(\rho_3, 0)$, and its nearby trajectories are far away from this point. When $z \to +\infty$,there are several spiral trajectories close to saddle point $(\rho_3, 0)$ and tend to focus $(\rho_2, 0)$; when $z \to -\infty$,these trajectories are far away from the focus and eventually tend to infinity. It shows that when $z \to +\infty$,the system is stable at $(\rho_2, 0)$;when $z \to -\infty$,the system is unstable at $(\rho_2, 0)$, the trajectory can be regarded as the system saddle-focus-saddle point solution.

Figure 2 corresponds to the first situation in Table 1. Figure 2 also shows that the system is unstable at the equilibrium point $(\rho_1, 0)$. The spiral starting near (0.002,0) tends to focus $z \to +\infty$,at $(\rho_2, 0)$,and the system is stable at this point; when $z \to -\infty$, it is far away from focus $(\rho_2, 0)$,and the system is unstable.

5 Conclusion

In this paper, traveling wave substitution is used to study the type and stability of equilibrium solutions of the improved Bando macro model. For further analysis and comparison, this paper selects two groups of parameters to describe the global distribution structure of the trajectory near the equilibrium point on the phase plane. Then, the stability of these equilibrium points is analyzed and described in detail.

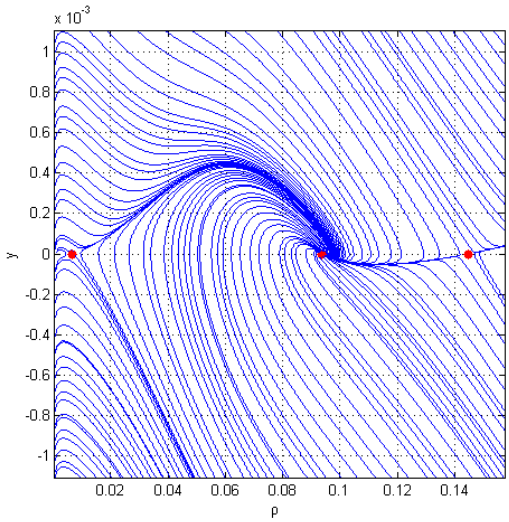

Fig. 1. Phase plane ρ - y trajectory diagram, where traveling wave velocity $c = -1.371$,traveling wave parameter $q_* = 0.2$.

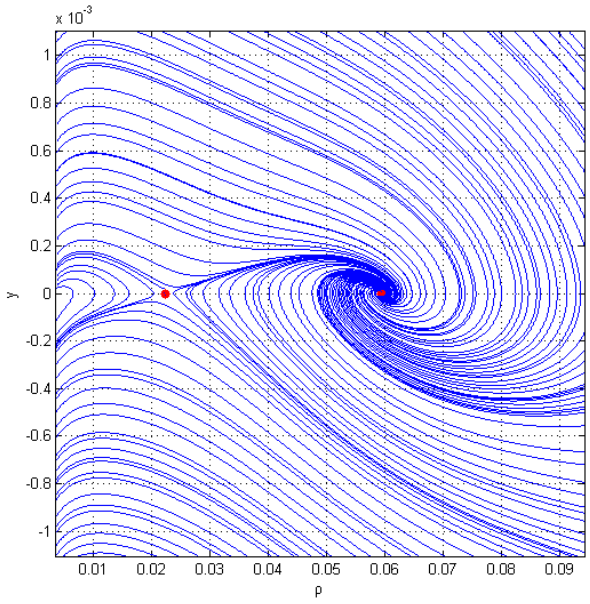

Fig. 2. Phase plane ρ - y trajectory diagram,where traveling wave velocity $c = -1.38$, traveling wave parameter $q_* = 0.64$.

The authors would like to thank the anonymous referees and the editor for their valuable opinions. This work is partially supported by the National Natural Science Foundation of China under the Grant No. 61863032 and the Natural Science Foundation of Gansu Province of China under the Grant No. 20JR5RA533 and the China Postdoctoral Science Foundation Funded Project (Project No.: 2018M633653XB) and the "Qizhi" Personnel Training Support Project of Lanzhou Institute of Technology (2018QZ-11) and Gansu Province Educational Research Project (Grant No. 2021A-166).

Reference

1. Pipes L A. An Operational Analysis of Traffic Dynamics[J]. Journal of Applied Physics, 1953, 24(3):274-281.
2. G.F. Newell. A simplified car-following theory: a lower order model[J]. Transportation Research Part B,2002,36(3):
3. M. Bando,K. Hasebe,A. Nakayama,A. Shibata,Y. Sugiyama. Dynamical model of traffic congestion and numerical simulation[J]. Physical review.E.Statistical physics, plasmas, fluids, and related interdisciplinary topics,1995,51(2):
4. Dirk Helbing,Benno Tilch. Generalized force model of traffic dynamics[J]. Physical Review E,1998,58(1):
5. Jiang R,Wu Q,Zhu Z. Full velocity difference model for a car-following theory.[J]. Physical review. E, Statistical, nonlinear, and soft matter physics,2001,64(1 Pt 2):
6. Richards P I. Shock Waves on the Highway[J]. Operations Research, 1956, 4(1):42-51.
7. Jian Zhang,Tie-Qiao Tang,Shao-Wei Yu. An improved car-following model accounting for the preceding car's taillight[J]. Physica A: Statistical Mechanics and its Applications,2018,492:
8. Liu Zhaoze,Cheng Rongjun,Ge Hongxia. Research on preceding vehicle's taillight effect and energy consumption in an extended macro traffic model[J]. Physica A: Statistical Mechanics and its Applications,2019,525: